

1 **A unique mode of nucleic acid immunity performed by a single multifunctional enzyme**

2

3 S. M. Nayeemul Bari<sup>1</sup>, Lucy Chou-Zheng<sup>1</sup>, Katie Cater<sup>1</sup>, Vidya Sree Dandu<sup>1</sup>, Alexander

4 Thomas<sup>1</sup>, Barbaros Aslan<sup>1</sup>, and Asma Hatoum-Aslan<sup>1\*</sup>

5 <sup>1</sup> Department of Biological Sciences, University of Alabama, Tuscaloosa, AL 35487, USA

6

7 **Organisms spanning all domains of life protect against pathogens using diverse**  
8 **mechanisms of nucleic acid immunity which detect and eliminate foreign genetic**  
9 **material<sup>1</sup>. The perpetual arms race between bacteria and their viruses (phages) has given**  
10 **rise to both innate and adaptive nucleic acid immunity mechanisms, including**  
11 **restriction-modification and CRISPR-Cas, respectively<sup>2</sup>. These sophisticated systems**  
12 **encode multiple components that sense and degrade phage-derived genetic material**  
13 **while leaving the host genome unharmed. Here, we describe a unique mode of innate**  
14 **immunity performed by a single protein, SERP2475, herein renamed to Nhi. We show that**  
15 **this enzyme protects against phages by preventing phage DNA accumulation, and in a**  
16 **purified system it degrades both DNA and RNA substrates. This enzyme also exhibits**  
17 **ATP-dependent helicase activity, and excess ATP abrogates nuclease function,**  
18 **suggesting a possible mechanism for its regulation. Further, using directed evolution, we**  
19 **isolated and characterized a collection of resistant phage mutants and found that a**  
20 **single-stranded DNA binding protein provides a natural means for phages to escape**  
21 **immunity. These observations support a model in which Nhi senses and degrades**  
22 **phage-specific replication intermediates. We also found that this dual-function enzyme**  
23 **protects against diverse phages, and its homologs are distributed across several**  
24 **bacterial phyla. Altogether, our findings reveal a new innate immune system with minimal**  
25 **composition that provides robust defense against diverse bacterial viruses.**

26

27           Phages are the most abundant entities in the biosphere<sup>3</sup>, and as such they impose a  
28 tremendous selective pressure upon their bacterial hosts. Phages attach to a specific host,  
29 inject their genome, and utilize the host's enzymes and energy stores to replicate exponentially,  
30 a process that typically leads to the death of the host (Fig. 1a). In response, bacteria have  
31 evolved diverse immune systems that target nearly every step of the phage infection cycle<sup>2</sup>--  
32 such systems may block phage genome entry, digest phage-derived nucleic acids, and/or  
33 initiate programmed cell death, a process known as abortive infection (Abi), to prevent the  
34 spread of a phage infection. Perhaps the most direct mechanism to block phage replication is  
35 through the use of nucleases that sense and destroy foreign genetic material. However, bacteria  
36 are known to possess only two modes of nucleic acid immunity which contribute to anti-phage  
37 defense: Innate immunity provided by restriction-modification (R-M) and adaptive immunity  
38 conferred by CRISPR-Cas (Fig. 1a). Given that bacteria and their phages have been co-  
39 evolving for billions of years, it is only natural to expect that many unknown immune systems  
40 are yet to be discovered, particularly in non-model organisms<sup>4,5</sup>.

41           Here, we sought to identify and characterize new anti-phage immune mechanisms in the  
42 commensal opportunistic pathogen *Staphylococcus epidermidis* RP62a<sup>6</sup>. This organism encodes  
43 a Type III-A CRISPR-Cas system<sup>7</sup>, an Abi mechanism<sup>8</sup>, and a putative Type I R-M system  
44 (GenBank Accession CP000029.1). All three systems reside within ~30,000 nucleotides of each  
45 other (Extended Data 1a), in agreement with recent evidence that suggests prokaryotic immune  
46 systems can be found clustered together within discrete defense islands<sup>5,9</sup>. Importantly, key  
47 insights into CRISPR-Cas and Abi in this organism were revealed by studying molecular  
48 interactions with the targets of immunity, siphophages  $\Phi$ NM1 and CNP<sub>x</sub>, respectively<sup>8,10</sup>.  
49 Therefore, we reasoned that the identification of novel immunity mechanisms would necessarily  
50 require the expansion of the *S. epidermidis* phage collection to include others unrelated to those  
51 commonly studied. Toward that end, we captured and characterized four new *S. epidermidis*  
52 podophages: Andhra, JBug18, Pontiff, and Pike<sup>12,13</sup>. These phages share over 95% sequence

53 identity (Extended Data 2), however, they exhibit distinct host ranges—While Andhra and Pontiff  
54 can infect the wild-type RP62a strain, JBug18 and Pike can only infect a mutant variant,  
55 LM1680<sup>14</sup>, which has lost the defense island and surrounding regions. These observations lead  
56 to the hypothesis that JBug18 and Pike are sensitive to genetic element(s) within the defense  
57 island.

58 To test this, we used a set of *S. epidermidis* RP62a mutants that bear deletions of varying  
59 extents across the defense island<sup>14</sup> (Extended Data 1a). These strains were plated together with  
60 Andhra and JBug18, representative phages with resistant and sensitive phenotypes, respectively.  
61 The resulting zones of bacterial growth inhibition (plaques) were enumerated, and the data  
62 revealed that only one of the deletion mutants encodes the gene(s) required for complete  
63 protection against JBug18. These observations narrowed down the protective genetic element(s)  
64 to a stretch of ~12,000 nucleotides containing 12 genes (*SERP2466-SERP2477*) which  
65 incidentally encompasses the R-M system (Extended Data 1b). To determine which of the 12  
66 gene(s) are responsible for immunity, they were inserted (individually and in groups) into a  
67 derivative of plasmid pC194<sup>15</sup> (herein referred to as p*SERP*-), introduced into *S. epidermidis*  
68 LM1680, and the resulting strains were challenged with Andhra and JBug18. Through this  
69 analysis, we found that a single gene of unknown function, *SERP2475*, is sufficient to provide  
70 robust immunity against both JBug18 (Extended Data 1 c and d) and Pike (Extended Data 3 a  
71 and b).

72 We next sought to characterize the mechanism of *SERP2475*-mediated immunity. An  
73 adsorption assay was first used to determine that JBug18 can attach to LM1680/p*SERP*-2475  
74 cells just as efficiently as can Andhra (Fig. 1b), thus ruling out an adsorption-blocking mechanism.  
75 A cell viability assay was next used to test for abortive infection. The prediction is that if  
76 programmed cell death accompanies immunity, then challenge with a high proportion of phages  
77 to cells ( $\geq 1:1$ ) would lead to significant cell death similar to that observed when there is no immune  
78 protection<sup>16,17</sup>. To test this, phages were combined with LM1680/p*SERP*-2475 cells in liquid media

79 at ratios of 1:1, 5:1, or 10:1, and cell viability was measured following 5 hours. We found that while  
80 Andhra causes significant death of LM1680/pSERP-2475 cells, JBug18 elicits only a minor  
81 decrease in the viability of this strain, even when phages outnumber bacteria 10:1 (Fig. 1c). These  
82 observations indicate that abortive infection is unlikely to be occurring. Finally, quantitative PCR  
83 (qPCR) was used to track the accumulation of phage DNA at various time points following  
84 infection. The results showed that while Andhra's DNA accumulates to ~20-fold by 20 minutes  
85 post-adsorption in LM1680/pSERP-2475, JBug18's DNA accumulates to less than 4-fold in the  
86 same time period (Fig. 1d). These observations support the hypothesis that SERP2475 interferes  
87 with phage DNA replication and/or expression.

88 SERP2475 encodes a 606 amino acid protein with predicted ATPase and helicase  
89 domains (according to BLASTp, Fig. 2a). Additionally, the HH Pred homology search tool<sup>18</sup>  
90 identified similarities between the N-terminus of SERP2475 and the HsdR restriction  
91 endonuclease from *Vibrio vulnificus*. Finally, the I-TASSER structure prediction tool<sup>19</sup> showed  
92 potential similarities with the eukaryotic DNA2 nuclease-helicase<sup>20</sup>. To test the importance of  
93 these predicted activities *in vivo*, two mutant versions of pSERP-2475 were created, -mutA and -  
94 mutB, which encode multiple amino acid substitutions in the predicted nuclease and helicase  
95 active sites, respectively (Fig. 2a). Following challenge with phage, we found that JBug18 could  
96 now replicate on both strains (Extended Data 4), indicating that both regions of the protein are  
97 required for immune function *in vivo*.

98 To test for its activities *in vitro*, SERP2475 and both mutants were overexpressed in *E.*  
99 *coli* and purified (Fig. 2b). The proteins were first combined with single-stranded DNA and RNA  
100 substrates (Extended Data 5a) and various divalent cations to test nuclease activity, and we  
101 observed that SERP2475 can indeed degrade both substrates in the presence of Mg<sup>2+</sup> or Mn<sup>2+</sup>  
102 (Extended Data 5 b and c). Importantly, this activity is significantly abrogated in both mutants (Fig.  
103 2c), confirming that the activity stems from SERP2475. Similar nuclease assays using circular  
104 single-stranded DNA and RNA substrates revealed that a free end is required for nuclease activity

105 (Extended Data 6 a and b). Finally, we tested DNase activity on various double-stranded  
106 substrates (Extended Data 7), and found that while the enzyme is unable to degrade double-  
107 stranded DNA with blunt ends, it can cut short stretches of double-stranded DNA (albeit  
108 inefficiently), particularly if provided with a 3'- overhang (Fig. 2d). Altogether, these results  
109 demonstrate that SERP2475 is primarily a 3'-5' exonuclease with a strong preference for single-  
110 stranded nucleic acids.

111 We next tested for ATPase and helicase activities. SERP2475 is a predicted superfamily  
112 1 helicase (pfam01443), which functions as a monomer or dimer to unwind double-stranded  
113 substrates using energy from ATP<sup>21</sup>. An ATPase assay showed that SERP2475 does in fact  
114 hydrolyze ATP (Fig. 2e). A helicase assay was next performed by incubating the enzyme with  
115 ATP and various DNA substrates, and the results showed that SERP2475 can indeed unwind  
116 double-stranded DNA, particularly when offered a 5'- or 3'- overhang (Fig. 2f). Interestingly, the  
117 single-stranded product released upon unwinding remains intact in the helicase assay, suggesting  
118 that excess ATP may have an inhibitory effect on nuclease activity. To test this, the nuclease  
119 assays were repeated in the presence of ATP, and we found that ATP inhibits nuclease activity  
120 in a dose-dependent manner (Fig. 2g). Altogether, these results demonstrate that SERP2475  
121 exhibits both nuclease and helicase activities that likely compete with one another. In addition,  
122 given that ATP drives helicase activity while inhibiting nuclease activity, we hypothesize that ATP  
123 levels may provide a mechanism for functional regulation of the enzyme.

124 To refine our understanding of this mechanism, we sought to determine how Andhra  
125 escapes immunity. Andhra and JBug18 encode the same 20 protein homologs (Extended Data  
126 8a) and an alignment of their coding regions show that they differ at only 705 positions by either  
127 a single-nucleotide polymorphism (SNP) or a gap (Supplementary file 1). To narrow down which  
128 SNPs and/or gaps in Andhra are important for resistance to immunity, we first attempted to isolate  
129 naturally-evolved JBug18 mutants that can escape immunity by plating concentrated phage  
130 preparations with LM1680/pSERP-2475. After several failed attempts at recovering plaques, one

131 attempt yielded resistant phages, which upon further inspection were found to possess hybrid  
132 genomes that contain a patchwork of Andhra and JBug18 sequences. These hybrids necessarily  
133 arose through the inadvertent mixing of the two phages. Nonetheless, this fortuitous accident  
134 proved invaluable in helping to pinpoint the region required for immune resistance--since all  
135 hybrids can escape immunity, they must share Andhra-derived sequences in the region required  
136 for resistance. Therefore, we purified and sequenced eight such hybrids, and determined the  
137 fraction of hybrids that possess Andhra identity at each of the 705 differing positions across their  
138 coding regions. We found that all eight hybrids share Andhra identity at positions 891-2117 in the  
139 alignment (Fig. 3a and Supplementary file 1). This region overlaps gene products (*gp*) 03-06 in  
140 the phage genomes and encompasses 69 SNPs and gaps, of which, 64 are concentrated within  
141 *gp03* and *gp04* (Fig. 3b). Accordingly, we speculated that one or both of the latter are responsible  
142 for resistance.

143         To narrow down the protective region even further, a second set of resistant JBug18  
144 hybrids were generated which bear Andhra-derived sequences in *gp03* and *gp04*. This was  
145 accomplished by introducing Andhra's *gp03* and/or *gp04* coding regions into *S. epidermidis*  
146 LM1680 on plasmids, and then propagating JBug18 on these strains to allow the phage to  
147 recombine with the Andhra-derived sequences (Extended Data 8b). The resulting phages were  
148 then plated on LM1680/p*SERP-2475* to select for resistant phage recombinants. Ten such hybrids  
149 (9-18) were purified, and sequencing across *gp03* and *gp04* revealed that they had all acquired  
150 a 60-nucleotide stretch spanning positions 1302-1362 in Andhra's genome (Fig. 3c and  
151 Supplementary file 2). This region overlaps *gp03*, which encodes a single-stranded DNA binding  
152 protein (SSB, Fig 3d, and Supplementary file 2). Importantly, JBug18 harbors a 5-nucleotide  
153 insertion in this region and consequently harbors a truncated SSB (Fig. 3d and Extended Data  
154 8c). However, by acquiring the 60-nucleotide stretch from Andhra, all ten hybrids had restored  
155 the reading frame and hence encode a full-length SSB, suggesting that the SSB C-terminus is  
156 essential for escape from immunity. In agreement with these observations, Pontiff and Pike

157 possess the expected *gp03* genotypes: While the resistant phage Pontiff encodes a full-length  
158 SSB, the sensitive phage Pike encodes a truncated version, this time due to a single nucleotide  
159 deletion (Extended Data 8d). Since SSBs are known to bind and protect DNA and regulate the  
160 replication machinery<sup>23</sup>, our observations support a preliminary model for immunity in which  
161 SERP2475 senses phage-specific replication intermediates and uses its helicase and nuclease  
162 activities to unwind and degrade them (Fig. 4). Future work will investigate how these activities  
163 are coordinated to achieve anti-phage defense.

164 Altogether, our findings describe a new mechanism of innate nucleic acid immunity  
165 performed by *S. epidermidis* RP62a SERP2475. Taking into account its demonstrated functions,  
166 we propose to name this enzyme Nhi (Nuclease-helicase mediated immunity). Importantly, further  
167 testing has revealed that Nhi provides robust immunity against diverse phages that infect both *S.*  
168 *epidermidis* and *S. aureus* strains (Extended Data 9). Additionally, Nhi homologs can be found in  
169 several bacterial phyla (Extended Data 10). Thus, this unique mode of innate immunity likely  
170 represents a common defense strategy used in the battle between bacteria and their viruses.

171

## 172 **Methods**

173 **Bacterial strains and growth conditions.** *S. epidermidis* RP62a and mutant variants were a  
174 generous gift from Luciano Marraffini. *S. epidermidis* strains were grown in Brain Heart Infusion  
175 (BHI, BD Diagnostics), *S. aureus* strains were grown in Tryptic Soy Broth (TSB, BD  
176 Diagnostics), *E. coli* DH5 $\alpha$  was grown in Luria Bertani (LB) broth (VWR), and *E. coli* Rossetta2  
177 (DE3) was grown in Terrific broth (VWR) for protein purification. Growth media was  
178 supplemented with the following: 10  $\mu$ g/ml chloramphenicol (to select for pC194-based  
179 plasmids), 10  $\mu$ g/ml tetracycline (to select pT181-based plasmids), 15  $\mu$ g/ml neomycin (to select  
180 for *S. epidermidis* cells), 30  $\mu$ g/ml chloramphenicol (to select for *E. coli* Rossetta2 plasmids) and  
181 50  $\mu$ g/ml kanamycin (to select for pET28b-His<sub>10</sub>Smt3-based plasmids).



182 **Phage propagation and plate infection assays.** *S. epidermidis* phages (Andhra, JBug18,  
183 Pontiff, Pike, Quidividi, and Twillingate) and *S. aureus* phages (ISP, Lorac, and Pabna) were  
184 propagated on their respective hosts to create stocks. Stock concentrations in plaque-forming  
185 units per mL (pfu/mL) were determined as previously described<sup>12,13,24,25</sup>. For plate infection  
186 assays, 10-fold dilutions of phage stocks were spotted atop a lawn of indicated strains using the  
187 double-agar overlay method<sup>12</sup>. Following overnight incubation, phage pfu/mL were enumerated.

188 **Construction of pC194 and pT181-based plasmids and introduction into staphylococcal**  
189 **strains.** All pC194- and pT181- based plasmids were constructed using either inverse PCR or  
190 Gibson Assembly<sup>26</sup> with the primers listed in Table S1 as described previously<sup>27</sup>. pAH011<sup>28</sup>, a  
191 derivative of pC194<sup>15</sup>, was used as the backbone for plasmids designated as pSERP- in this  
192 study. Plasmid pT181<sup>22</sup> was used as backbone for pT181-*gp03* and pT181-*gp0304*. All  
193 assembled plasmids were first introduced into *S. aureus* RN4220 (pC194-based plasmids) or  
194 OS2 (pT181-based plasmids) via electroporation and inserted sequences were confirmed by  
195 PCR amplification and Sanger sequencing (performed by Eurofins MWG Operon) using primers  
196 shown in Table S1. Confirmed plasmids were purified using EZNA Plasmid Mini Kit (Omega  
197 Bio-tek), and where indicated, introduced into *S. epidermidis* LM1680 via electroporation as  
198 previously described<sup>27</sup>.

199 **Phage adsorption and cell viability assays.** Overnight cultures of *S. epidermidis*  
200 LM1680/pSERP-NC and LM1680/pSERP-2475 were diluted 1:100 in fresh BHI supplemented  
201 with antibiotics and 5 mM CaCl<sub>2</sub>, and incubated at 37°C with agitation for one hour. For the  
202 adsorption assay, Andhra or JBug18 were added to cultures (0.01:1 phage:cell ratio) and  
203 incubated at 37°C for 10 min. Cells along with adsorbed phages were pelleted at 8000 x g for 5  
204 min at 4°C and resulting supernatants were passed through 0.45 µm syringe filter. The number  
205 of free phages in the supernatants were enumerated by the double-agar overlay method<sup>12</sup>. The  
206 number of adsorbed phages were determined by subtracting the number of phages in



207 suspension from the number that was initially added. Triplicate samples were prepared for each  
208 treatment, and two independent trials were conducted. For cell viability assays, 200  $\mu\text{l}$  of the  
209 bacterial cultures were distributed into a 96-well microtiter plate (into triplicate wells for each  
210 treatment), and phages were added to cells at ratios of 1:1, 5:1, or 10:1. These bacteria-phage  
211 mixtures were incubated at 37°C with agitation for an additional five hours. 25  $\mu\text{l}$  of 0.1% (w/v)  
212 2,3,5 Triphenyltetrazolium chloride (TTC) was added into each well and the microtiter plate was  
213 incubated at 37°C for an additional 30 mins to allow the colorless TTC to become enzymatically  
214 reduced to the red 1,3,5-triphenylformazan product by actively growing bacterial cells. The  
215 relative numbers of viable cells were then determined by measuring the absorbance at 540 nm.  
216 Triplicate measurements were averaged, and two independent trials were conducted.

217 **Phage infection time course followed by quantitative PCR.** Phage infection time course  
218 assays were conducted in liquid media as previously described<sup>29</sup>. Briefly, *S. epidermidis*  
219 LM1680 mid-log cells bearing *pSERP-NC* or *pSERP-2475* were infected with Andhra or JBug18  
220 (phage:cell ratio of 0.5:1), cells were harvested at 0, 10, or 20 minutes post-infection, and their  
221 total DNA was extracted. Each qPCR reaction (25  $\mu\text{L}$ ) contained 500 ng of total DNA as  
222 template, 0.4 nM of phage-specific primers (N233 and N234) or host-specific primers (S001 and  
223 S002) (Table S1), and 1X PerfeCTa SYBR Green SuperMix (Quanta Biosciences). Separate  
224 standard reactions containing  $10^2$ – $10^9$  DNA molecules were also prepared using purified Andhra  
225 phage DNA extract, JBug phage DNA extract, or bacterial genomic DNA extract. A CFX  
226 Connect Real-Time PCR Detection System (Bio-Rad) was used to amplify the DNA templates.  
227 Phage DNA copy number was normalized against host values, and the normalized value for the  
228 0 min time point was set to one to obtain the relative DNA abundance for the rest of the time  
229 points as described previously<sup>29</sup>. Triplicate measurements were taken for each of two  
230 independent trials.

231 **Construction of pET28b-His<sub>10</sub>Smt3-based plasmids.** pET28b-His<sub>10</sub>Smt3-*SERP2475* was  
232 constructed using restriction cloning with primers N284 and N266 (Table S1) as previously  
233 described<sup>27</sup>. The ligated construct was introduced into *E. coli* DH5α by heat shock, and  
234 transformants were confirmed to have the desired plasmids using PCR and DNA sequencing  
235 with primers T7P and T7T (Table S1). Confirmed plasmids were purified using the EZNA  
236 Plasmid Mini Kit and introduced into *E. coli* Rosetta2 (DE3) cells for protein purification.  
237 Plasmids pET28b-H<sub>10</sub>Smt3-*SERP2475-mutA* and pET28b-H<sub>10</sub>Smt3-*SERP2475-mutB* were  
238 constructed by inverse PCR as described previously<sup>27</sup> using pET28b-His<sub>10</sub>Smt3-*SERP2475* as  
239 the backbone and primers listed in Table S1.

#### 240 **Purification of recombinant SERP2475, SERP2475-mutA, and SERP2475-mutB.**

241 Recombinant proteins encoded in pET28b-His<sub>10</sub>Smt3-based plasmids were overexpressed and  
242 purified as described previously<sup>29</sup>.

243 **Nuclease assays.** Single stranded RNA or DNA substrates were labeled on their 5'-ends by  
244 incubating with T4 polynucleotide kinase and  $\gamma$ -[<sup>32</sup>P]-ATP and purified over a G25 column (IBI  
245 Scientific). Double-stranded DNA duplexes were prepared by combining 5'-radiolabeled ssDNA  
246 oligonucleotides and unlabeled complementary ssDNA oligonucleotides (as shown in Fig. S6) in  
247 a 1:1.5 molar ratio. The mixtures were heated to 95°C for 5 min and then slowly cooled down to  
248 room temperature over a period of 3 hours. Circular ssRNA was prepared by incubating the  
249 radiolabeled substrate with T4 RNA ligase 1 (NEB) and the supplied buffer according to the  
250 manufacturer's instructions. For nuclease assays, radiolabeled substrates were combined with  
251 25 pmol of enzyme in nuclease buffer (25 mM Tris-HCl pH 7.5, 2 mM DTT) supplemented with  
252 10 mM of divalent metal (MgCl<sub>2</sub>, MnCl<sub>2</sub>, NiCl<sub>2</sub> or ZnCl<sub>2</sub>), EDTA, or ATP as indicated in figures  
253 and legends. Reactions were allowed to proceed at 37°C for indicated time periods. Reactions  
254 were stopped by adding an equal volume of 95% formamide loading buffer and resolved using  
255 denaturing PAGE. Gels were exposed to a Storage Phosphor screen and visualized using a  
256 Typhoon FLA 9500 biomolecular imager.

257 **Helicase Assay.** Double-stranded DNA substrates with the top strand radiolabeled were  
258 prepared as described above. The helicase assay was performed by first mixing 10 pmol of  
259 radiolabeled DNA duplex with a 5-fold molar excess of unlabeled top-strand DNA. This mixture  
260 was combined with 25 pmol SERP2475 in nuclease buffer supplemented with 10 mM MgCl<sub>2</sub> and  
261 20 mM ATP. Reaction mixtures were incubated at 37°C for 1h. As a positive control, DNA  
262 substrates were heated to 95°C for 15 min in the absence of the enzyme. Samples were  
263 resolved on an 8% (v/v) non-denaturing polyacrylamide gel. The gel was dried under vacuum at  
264 80°C, exposed to a Storage Phosphor screen and visualized by a Typhoon FLA 9500  
265 biomolecular imager. Three independent trials were conducted.

266 **ATPase assay.** A Quanticrom™ ATPase/GTPase Assay kit (BioAssay Systems) was used  
267 according to the manufacturer's protocol with some minor modifications. Briefly, 40 µl reactions  
268 were set up in triplicate in a 96-well plate. Reaction wells contained 0.5 X assay buffer, 50 pmol  
269 enzyme, and 50 µM ATP. Control wells without enzyme were supplemented with protein dialysis  
270 (IMAC) buffer<sup>29</sup>. Reaction wells containing known concentrations of inorganic phosphate were  
271 also prepared to generate a standard curve. The microtiter plate was incubated at 37°C for 1 h,  
272 and 200 µl of stop reagent was added to each well. The plate was incubated for an additional 30  
273 min at room temperature, and absorbance at 620 nm was measured with a Spectramax M2  
274 microplate reader (Molecular Devices). The concentration of free phosphate was calculated by  
275 plotting the OD<sub>620</sub> value against the standard curve. The fraction of ATP consumed in the  
276 reaction was calculated by dividing the molar amount of free phosphate generated by the molar  
277 amount of ATP in the initial reaction. Triplicate wells were prepared for each treatment, and  
278 three independent trials were conducted.

279 **Phage hybrid generation and sequencing.** JBug18-Andhra Hybrids 1-8 were isolated as  
280 immune resistant mutants following challenge of LM1680/pSERP-2475 with a high titer lysate of  
281 JBug18 (~1 x 10<sup>10</sup> pfu/mL). To generate JBug18-Andhra Hybrids 9-18, overnight cultures of S.

282 *epidermidis* LM1680 harboring pT181-*gp03* or pT181-*gp0304* were diluted 1:100 in fresh TSB  
283 supplemented with antibiotics and 5 mM CaCl<sub>2</sub>. The mixture was incubated at 37°C for an hour  
284 with agitation, then JBug18 was added to the cells in a 1:1 ratio, and the incubation continued  
285 with agitation overnight. The next day, cells were pelleted by centrifugation at 8000 x g for 5 min  
286 and supernatant was filtered through 0.45 µm filter. Filtered lysates were mixed with LM1680-  
287 p*SERP2475* overnight culture (1:1) and the mixture was plated on TSA containing 5 mM CaCl<sub>2</sub>  
288 using the double-agar overlay method<sup>12</sup>. For all phage hybrids, individual plaques were isolated  
289 and re-plated three times on LM1680/p*SERP-2475* to purify. Phages were propagated and their  
290 DNA was extracted as previously described<sup>30</sup>. Phage genomes were PCR amplified across the  
291 entire coding region for Hybrids 1-8 or *gp03-gp04* for Hybrids 9-18, and the PCR products were  
292 sequenced by the Sanger method (at Eurofins MWG Operon) using the primers listed in Table  
293 S1.

294 **Hybrid phage genome sequence analysis.** For JBug18-Andhra Hybrids 1-8, Sanger  
295 sequencing reads covering their coding regions were manually assembled using SnapGene  
296 software. For JBug18-Andhra Hybrids 9-18, a single read covered the region of interest,  
297 therefore no assembly was required. Sequences for each set of hybrids (1-8 and 9-18) were  
298 aligned with corresponding genomic regions in Andhra and JBug18 using the Clustal Omega  
299 Multiple Sequence Alignment tool (<https://www.ebi.ac.uk/Tools/msa/clustalo/>). The sequence  
300 alignments (Supplementary files 1 and 2) were analyzed by a Python script developed in-house  
301 which first scans the alignment of JBug18 and Andhra, identifies each position of non-similarity,  
302 and then determines at those positions the fraction of hybrids that possess Andhra identity. The  
303 output data was exported into an Excel file, and the graphs showing the fraction of hybrids with  
304 Andhra identity at each position were generated using Microsoft Excel.

305 **Data availability.** The raw phage sequence reads that support the findings of Figure 4 are  
306 publicly available through figshare (10.6084/m9.figshare.9598040). The Accession codes for  
307 Andhra, JBug18, Pontiff, and Pike genomes are KY442063, MH972263, MH972262, and

308 MH972261, respectively. Phages, mutant derivatives, and constructs can be made available  
309 upon written request.

310 **Code availability.** The Python code written to analyze the data for Figure 4 is freely available at

311 GitHub (<https://github.com/ahatoum/Hybrid-phage-genome-sequence-analysis>).

312 **References**

- 313 1. Hartmann, G. *Nucleic Acid Immunity. Advances in Immunology* **133**, (Elsevier Inc., 2017).
- 314 2. Rostøl, J. T. & Marraffini, L. (Ph)ighting Phages : How Bacteria Resist Their Parasites.  
315 *Cell Host Microbe* **25**, 184–194 (2019).
- 316 3. Bergh, O., Børsheim, K. Y., Bratbak, G. & Heldal, M. High abundance of viruses found in  
317 aquatic environments. *Nature* **340**, 467–468 (1989).
- 318 4. Stern, A. & Sorek, R. The phage-host arms race: Shaping the evolution of microbes.  
319 *BioEssays* **33**, 43–51 (2011).
- 320 5. Doron, S. *et al.* Systematic discovery of antiphage defense systems in the microbial  
321 pangenome. *Science*. **359**, eaar4120 (2018).
- 322 6. Christensen, G. D., Baddour, L. M. & Simpson, W. A. Phenotypic variation of  
323 *Staphylococcus epidermidis* slime production in vitro and in vivo. *Infect. Immun.* **55**,  
324 2870–2877 (1987).
- 325 7. Marraffini, L. A. & Sontheimer, E. J. CRISPR interference limits horizontal gene transfer  
326 in staphylococci by targeting DNA. *Science*. **322**, 1843–1845 (2008).
- 327 8. Depardieu, F. *et al.* A Eukaryotic-like Serine/Threonine Kinase Protects Staphylococci  
328 against Phages. *Cell Host Microbe* **20**, 471–481 (2016).
- 329 9. Makarova, K. S., Wolf, Y. I., Snir, S. & Koonin, E. V. Defense Islands in Bacterial and  
330 Archaeal Genomes and Prediction of Novel Defense Systems. *J. Bacteriol.* **193**, 6039–  
331 6056 (2011).
- 332 10. Goldberg, G. W., Jiang, W., Bikard, D. & Marraffini, L. A. Conditional tolerance of  
333 temperate phages via transcription-dependent CRISPR-Cas targeting. *Nature* **514**, 633–  
334 637 (2014).
- 335 11. Deghorain, M. & Van Melder, L. The staphylococci phages family: An overview.  
336 *Viruses* **4**, 3316–3335 (2012).
- 337 12. Cater, K. *et al.* A Novel Staphylococcus Podophage Encodes a Unique Lysin with

- 338 Unusual Modular Design. *mSphere* **2**, 1–9 (2017).
- 339 13. Culbertson, E. K. *et al.* Draft Genome Sequences of Staphylococcus Podophages  
340 JBug18, Pike, Pontiff, and Pabna. *Microbiol. Resour. Announc.* **8**, e00054-19 (2019).
- 341 14. Jiang, W. *et al.* Dealing with the Evolutionary Downside of CRISPR Immunity: Bacteria  
342 and Beneficial Plasmids. *PLoS Genet.* **9**, e1003844 (2013).
- 343 15. Ehrlich, S. D. Replication and expression of plasmids from *Staphylococcus aureus* in  
344 *Bacillus subtilis*. *Proc. Natl. Acad. Sci. U. S. A.* **74**, 1680–1682 (1977).
- 345 16. Goldfarb, T. *et al.* BREX is a novel phage resistance system widespread in microbial  
346 genomes. *Embo J* **34**, 169–183 (2015).
- 347 17. Ofir, G. *et al.* DISARM is a widespread bacterial defence system with broad anti-phage  
348 activities. *Nat. Microbiol.* **3**, 90–98 (2017).
- 349 18. Zimmermann, L. *et al.* A Completely Reimplemented MPI Bioinformatics Toolkit with a  
350 New HHpred Server at its Core. *J. Mol. Biol.* **430**, 2237–2243 (2018).
- 351 19. Yang, J. *et al.* The I-TASSER Suite: protein structure and function prediction. *Nat.*  
352 *Methods* **12**, 7–8 (2015).
- 353 20. Zhou, C., Pourmal, S. & Pavletich, N. P. Dna2 nuclease-helicase structure, mechanism  
354 and regulation by Rpa. *Elife* **4**, e09832 (2015).
- 355 21. Fairman-Williams, M. E., Guenther, U.-P. & Jankowsky, E. SF1 and SF2 helicases: family  
356 matters. *Curr. Opin. Struct. Biol.* **20**, 313–324 (2010).
- 357 22. Khan, S. A., Carleton, S. M. & Novick, R. P. Replication of plasmid pT181 DNA in vitro :  
358 Requirement for a plasmid-encoded product. *Proc. Natl. Acad. Sci.* **78**, 4902–4906  
359 (1981).
- 360 23. Shereda, R. D. *et al.* SSB as an Organizer / Mobilizer of Genome Maintenance  
361 Complexes. *Crit. Rev. Biochem. Mol. Biol.* **43**, 289–318 (2008).
- 362 24. Freeman, M. E. *et al.* Complete Genome Sequences of *Staphylococcus epidermidis*  
363 Myophages Quidividi, Terranova, and Twillingate. *Microbiol. Resour. Announc.* **8**,



- 364 e00598-19 (2019).
- 365 25. Marc, A. *et al.* Complete Genome Sequence of *Staphylococcus aureus* Siphophage  
366 Lorac. *Microbiol. Resour. Announc.* **8**, e00586-19 (2019).
- 367 26. Gibson, D. G. *et al.* Enzymatic assembly of DNA molecules up to several hundred  
368 kilobases. *Nat Meth* **6**, 343–345 (2009).
- 369 27. Walker, F. C., Chou-Zheng, L., Dunkle, J. A. & Hatoum-Aslan, A. Molecular determinants  
370 for CRISPR RNA maturation in the Cas10 – Csm complex and roles for non-Cas  
371 nucleases. *Nucleic Acids Res.* **45**, 2112–2123 (2017).
- 372 28. Hatoum-Aslan, A., Maniv, I. & Marraffini, L. A. Mature clustered, regularly interspaced,  
373 short palindromic repeats RNA (crRNA) length is measured by a ruler mechanism  
374 anchored at the precursor processing site. *Proc. Natl. Acad. Sci.* **108**, 21218–21222  
375 (2011).
- 376 29. Chou-Zheng, L. & Hatoum-Aslan, A. A type III-A CRISPR-Cas system employs  
377 degradosome nucleases to ensure robust immunity. *Elife* 8:e45393 (2019).
- 378 30. Bari, S. M. N., Walker, F. C., Cater, K., Aslan, B. & Hatoum-Aslan, A. Strategies for  
379 Editing Virulent Staphylococcal Phages Using CRISPR-Cas10. *ACS Synth. Biol.* **6**,  
380 (2017).

381

## 382 **Supplementary Information**

383 The following supplementary files are also available:

384 Supplementary Table 1. Oligonucleotides used for cloning and PCR in this study.

385 Supplementary file 1. Multiple sequence alignment for JBug18-Andhra Hybrids 1-8

386 Supplementary file 2. Multiple sequence alignment for JBug18-Andhra Hybrids 9-18

387

## 388 **Acknowledgements**

389 AH-A would like to acknowledge funding for this project from the National Science Foundation  
390 CAREER award [MCB/1749886].

391

### 392 **Author Contributions**

393 S.M.N.B., L.C-Z, K.C., V.S.D., A.T., and B.A. performed experiments, S.M.N.B., L.C-G, B.A.,  
394 and A.H.-A. designed experiments, A.H.-A. conceived the study and wrote the manuscript, and  
395 all authors have read and approved the manuscript.

396

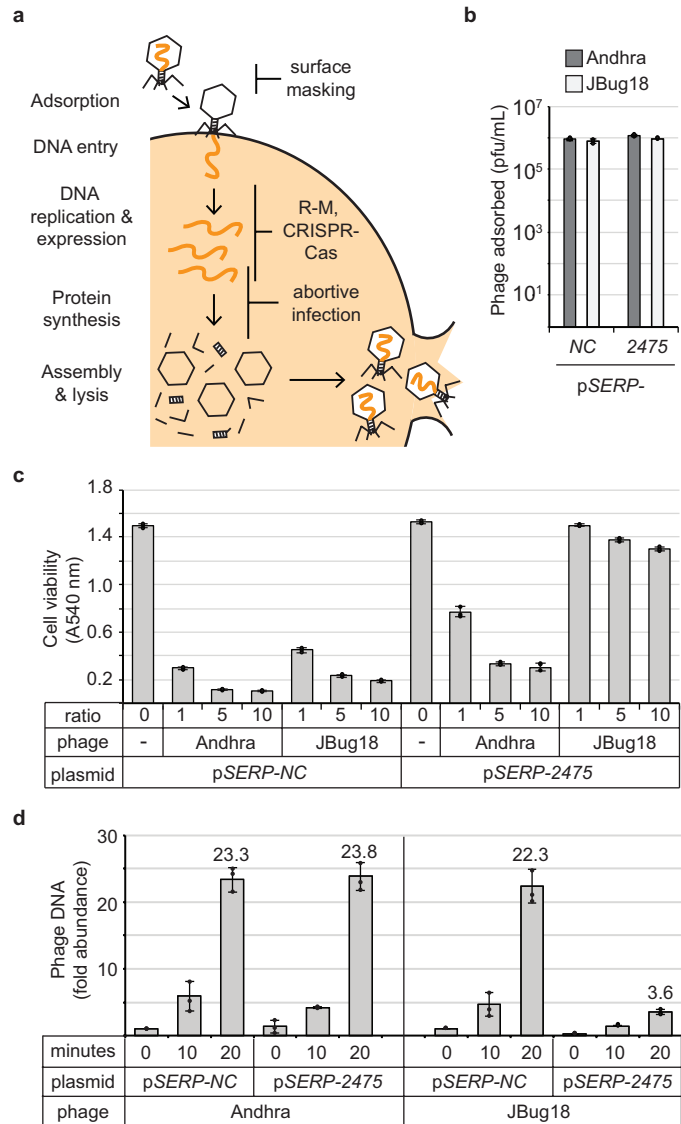
### 397 **Author Information**

398 The authors declare no conflict of interest. Correspondence and requests for materials should  
399 be addressed to A. H-A. (ahatoum@ua.edu).

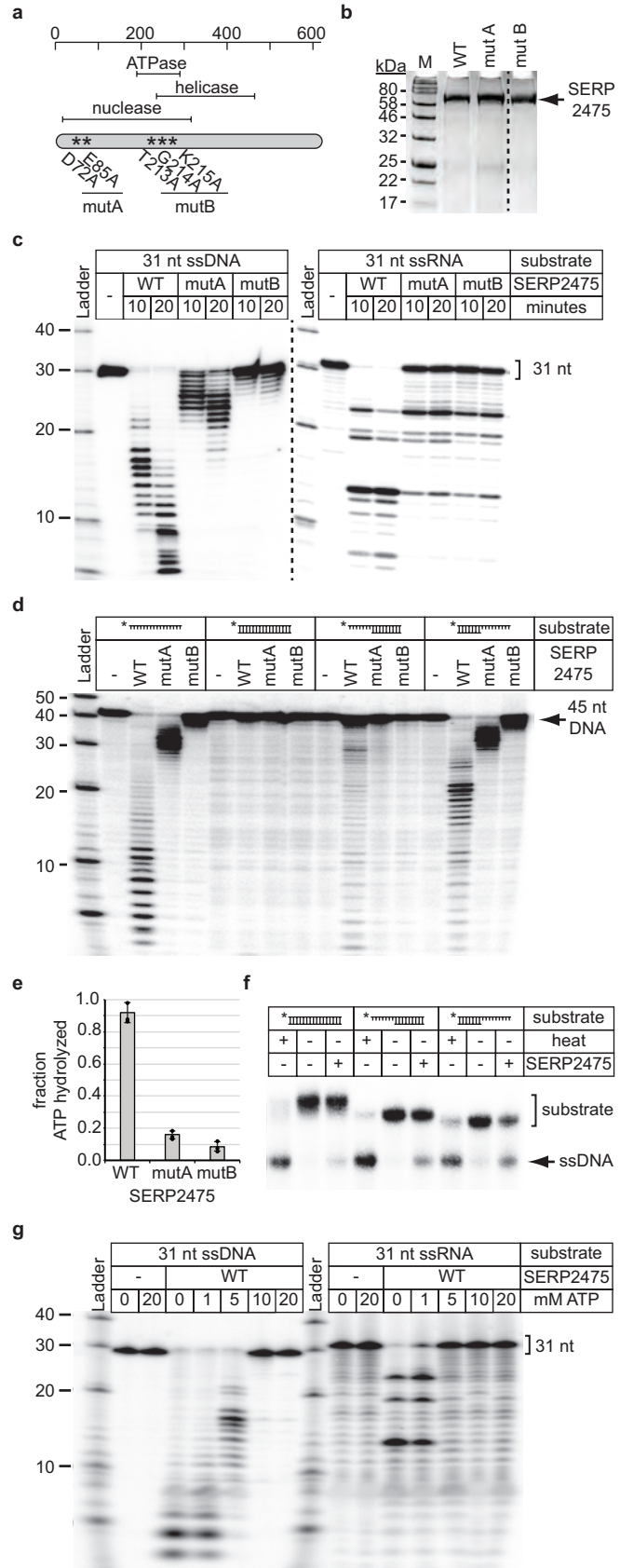
400 **Figures and Legends**

401 **Figure 1. SERP2475 impairs phage**

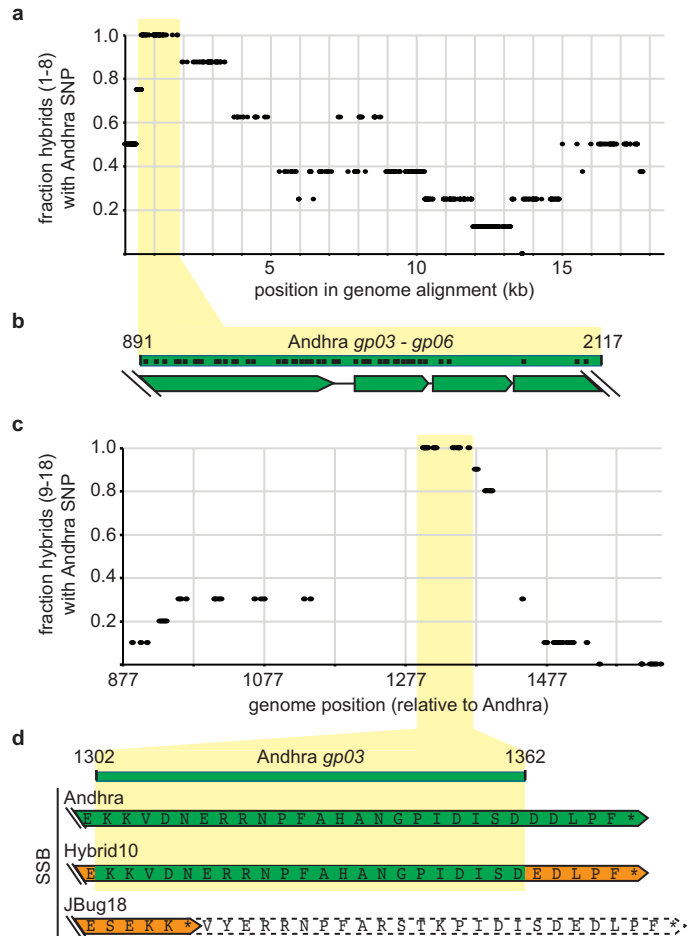
402 **DNA accumulation.** (a) Illustration of  
 403 the lytic phage replication cycle. Known  
 404 defense systems that interfere with each  
 405 step are indicated on the right. (b and c)  
 406 Results of an adsorption assay (b) and a  
 407 cell viability assay (c) following  
 408 challenge of *S. epidermidis* LM1680  
 409 cells bearing indicated plasmids with  
 410 Andhra and JBug18. (d) Relative  
 411 abundance of phage DNA at various  
 412 time points following phage infection as  
 413 measured by qPCR. For all experiments,  
 414 the mean  $\pm$  S.D. of triplicate  
 415 measurements are shown as a  
 416 representative of at least two  
 417 independent trials.



418 **Figure 2. SERP2475 exhibits nuclease,**  
 419 **ATPase, and helicase activities. (a)**  
 420 Predicted active sites of SERP2475 and  
 421 corresponding mutations introduced in this  
 422 study. **(b)** Purified recombinant  
 423 SERP2475 and mutant variants. **(c, d, and**  
 424 **g)** Nuclease assays in which SERP2475  
 425 and mutant variants were combined with  
 426 radiolabeled substrates and ATP where  
 427 indicated. **(e)** An ATPase assay with  
 428 indicated enzymes. Shown is an average  
 429 of triplicate measurements ( $\pm$ S.D.). **(f)** A  
 430 helicase assay in which SERP2475 was  
 431 combined with radiolabeled substrates  
 432 and 20 mM ATP. Dotted lines separate  
 433 data derived from different gels or non-  
 434 contiguous regions of the same gel. For all  
 435 assays, a representative of at least three  
 436 independent trials is shown.

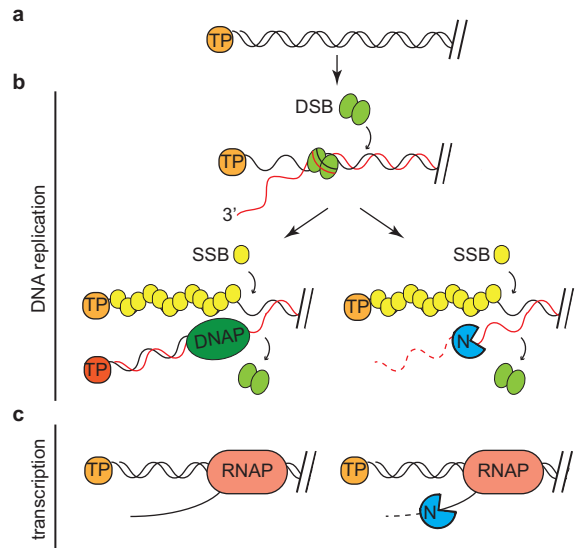


437 **Figure 3. A phage-encoded single-**  
 438 **stranded DNA binding protein protects**  
 439 **against immunity. (a and c) Fractions of**  
 440 **JBug18-Andhra Hybrids that harbor**  
 441 **Andhra identity at positions where the**  
 442 **parental phage genomes differ. Segments**  
 443 **common to all hybrids are highlighted in**  
 444 **yellow. (b and d) Expanded views of the**  
 445 **highlighted common regions. Black dots**  
 446 **in (b) indicate relative positions where**  
 447 **SNPs and/or gaps occur in an alignment**  
 448 **between the parental phages. In (d),**  
 449 **green and orange arrows with solid**  
 450 **borders delimit phage-encoded SSBs,**  
 451 **and the white arrow with dotted border**  
 452 **delimits a truncated portion.**

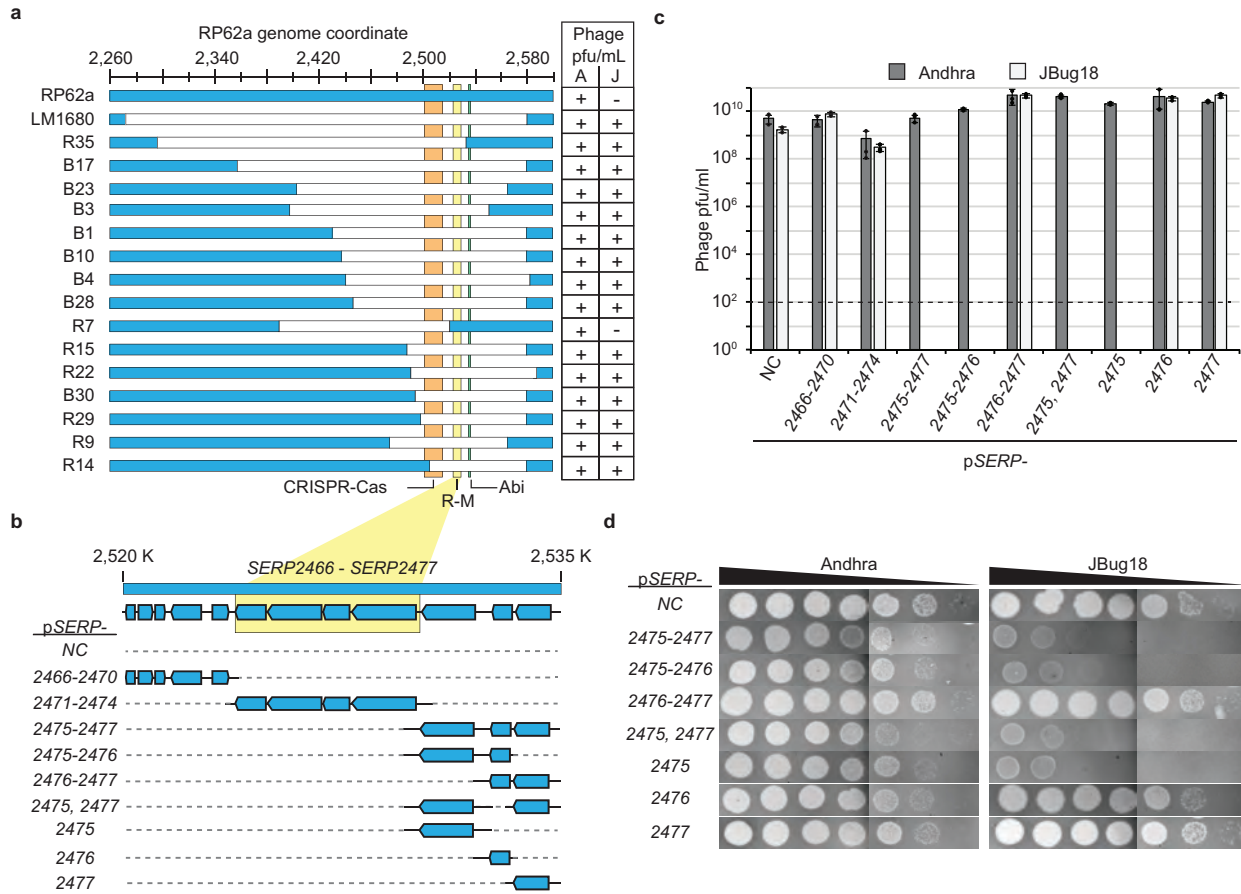


453  
 454  
 455  
 456  
 457  
 458  
 459  
 460  
 461

462 **Figure 4. Proposed mechanism for**  
463 **SERP2475 (Nhi) immunity.** (a) Image of the  
464 linear double-stranded genomic DNA of  
465 staphylococcal *Podoviridae* phages, in which  
466 each 5'-end is covalently linked to a terminal  
467 protein (TP). (b) During DNA replication, double-  
468 stranded DNA binding proteins (DSB) bind and  
469 unwind the DNA ends. Under normal  
470 circumstances (left) a DNA polymerase (DNAP)-  
471 TP complex binds to the free 3'-end and initiates DNA replication. However, in the presence of  
472 Nhi (N, right), the 3'-end is susceptible to unwinding/degradation by this enzyme. (c) Phage  
473 transcripts are also targeted by this enzyme. RNAP, RNA Polymerase.



474

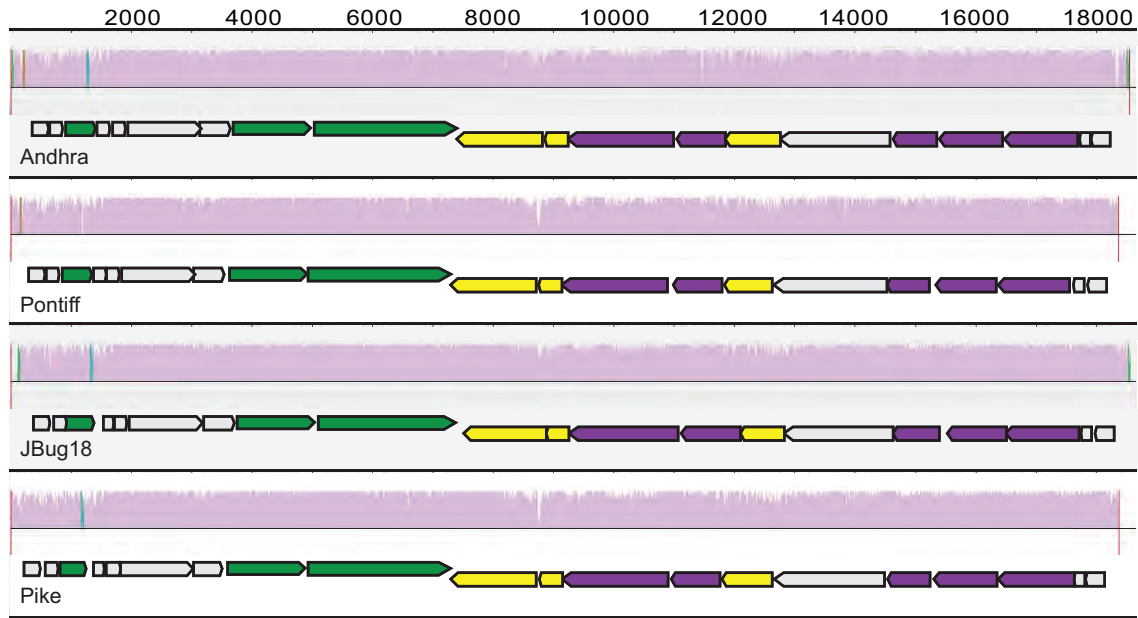


475

476

477 **Extended Data 1. SERP2475 provides robust immunity against phage JBug18.** (a) A  
 478 segment of the *S. epidermidis* RP62a genome and deletion mutants. Regions encoding  
 479 CRISPR-Cas, R-M, and Abi systems are highlighted. Strains were challenged with Andhra (A)  
 480 and JBug18 (J), and resulting plaque-forming units per milliliter (pfu/mL) are indicated: +, ~1 x  
 481 10<sup>9</sup> pfu/mL; -, 0 pfu/mL. (b) Magnified view of the genomic region responsible for immunity and  
 482 corresponding plasmids that were created. (c) *S. epidermidis* LM1680 strains harboring  
 483 indicated plasmids were challenged with phage, and the resulting pfu/mL are shown as an  
 484 average of triplicate measurements ( $\pm$  S.D.). The dotted line indicates the limit of detection. (d)  
 485 Representative plaque images following the application of ten-fold dilutions of Andhra and  
 486 JBug18 ( $1 \times 10^{-1}$  –  $1 \times 10^{-7}$ ) atop *S. epidermidis* LM1680 strains bearing indicated plasmids.





487      ■ DNA replication & packaging      ■ bacterial lysis      ■ structural protein      □ unknown function

488

489

490 **Extended Data 2. Four related *Podoviridae* phages with different host ranges.** Shown is a

491 multiple genome alignment of *S. epidermidis* podophages Andhra, Pontiff, JBug18, and Pike.

492 Genome coordinates are shown on top, and colored histograms indicate the nucleotide

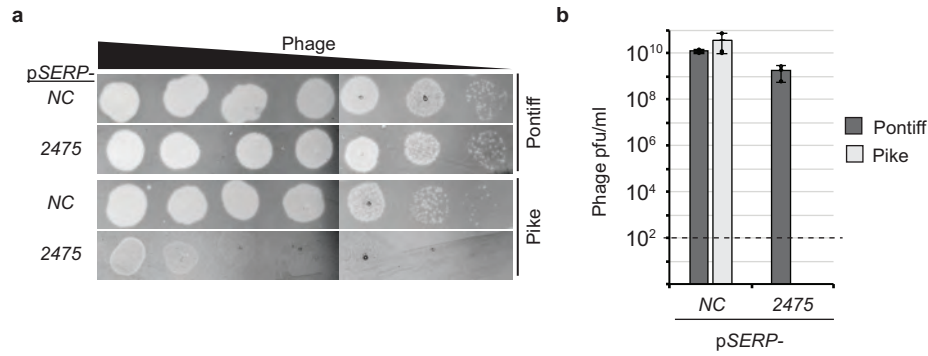
493 similarity at each position derived from a multiple sequence alignment. The open reading frames

494 for each phage are shown underneath the corresponding histogram. The histograms were

495 generated using the MAUVE open source software (<http://darlinglab.org/mauve/mauve.html>)

496 and the outlines of open reading frames from the MAUVE output were overlaid using Adobe

497 Illustrator.



498

499

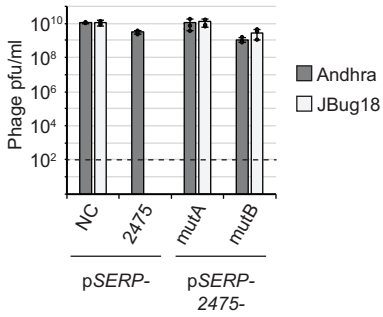
500 **Extended Data 3. SERP2475 is sufficient to provide robust protection against phage Pike.**

501 (a) 10-fold dilutions of phages Pontiff and Pike ( $1 \times 10^0 - 1 \times 10^{-6}$ ) were plated atop *S. epidermidis*

502 LM1680 cells bearing indicated plasmids. Shown are representative plate images for triplicate

503 experiments. (b) The average of triplicate plaque measurements ( $\pm$ S.D.) in pfu/mL. The dotted

504 line indicates the limit of detection for this assay.



505

506

507

508 **Extended Data 4. Accompanies Fig. 2. Predicted nuclease and ATP binding sites in**

509 **SERP2475 are required for immunity *in vivo*.** *S. epidermidis* LM1680 strains bearing the

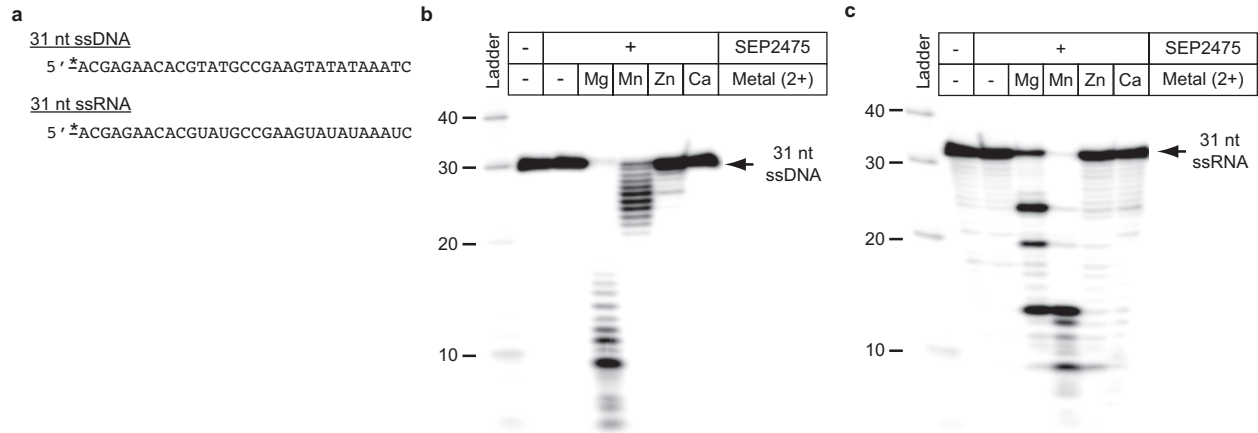
510 indicated plasmids were challenged with phages Andhra and JBug18, and resulting pfu/mL

511 were enumerated. While the pSERP-2475 -mutA plasmid encodes mutations in the predicted

512 nuclease active site, the -mutB plasmid encodes mutations in the predicted ATP binding domain

513 (see Fig. 2a for more details). Shown are an average of triplicate measurements ( $\pm$ S.D.). The

514 dotted line indicates the limit of detection for this assay.



515

516

517

518

519

520 **Extended Data 5. Accompanies Fig. 2. SERP2475 exhibits metal-dependent nuclease**

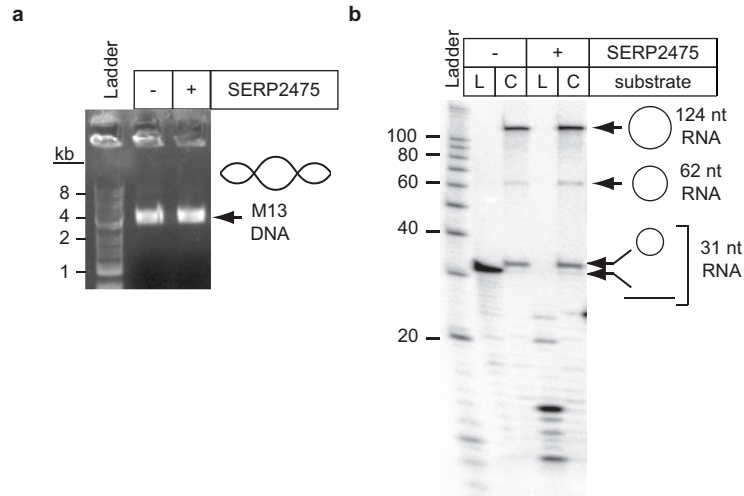
521 **activity.** (a) The 31-nucleotide single-stranded DNA and RNA substrates used for nuclease

522 assays in this figure and Fig. 2 panels (c) and (g). Asterisks indicate the position of the

523 radiolabel. (b and c) DNA and RNA substrates (respectively) were combined with SERP2475 in

524 nuclease buffer supplemented with indicated divalent metals. Shown are representative images

525 for three independent trials.



526

527

528

529

530 **Extended Data 6. Accompanies Fig. 2. SERP2475 cannot cut circular single-stranded**

531 **substrates.** Shown are nuclease assays in which SERP2475 was combined with indicated

532 single-stranded circular substrates. (a) For circular DNA, the reaction was supplemented with 10

533 mM MgCl<sub>2</sub> and the mixture was incubated at 37°C for 60 min. The reaction products were then

534 resolved on a 1% agarose gel. (b) For circular RNA, the reaction was supplemented with 10 mM

535 MnCl<sub>2</sub> and the mixture was incubated at 37°C for 20 min. The products were then resolved

536 using denaturing PAGE. L, linear; C, circular. Shown are representative images for two

537 independent trials.

538

45 nt ssDNA

5' \*TCACTTGGTACTAAATTAATACTATGTGATACACGATTATATTTTC

45 nt dsDNA

5' \*TCACTTGGTACTAAATTAATACTATGTGATACACGATTATATTTTC  
|||||  
AGTGAACCATGATTTAATTATGATACACTATGTGCTAATATAAAG

5' DNA overhang

5' \*TCACTTGGTACTAAATTAATACTATGTGATACACGATTATATTTTC  
|||||  
TGATACACTATGTGCTAATATAAAG

3' DNA overhang

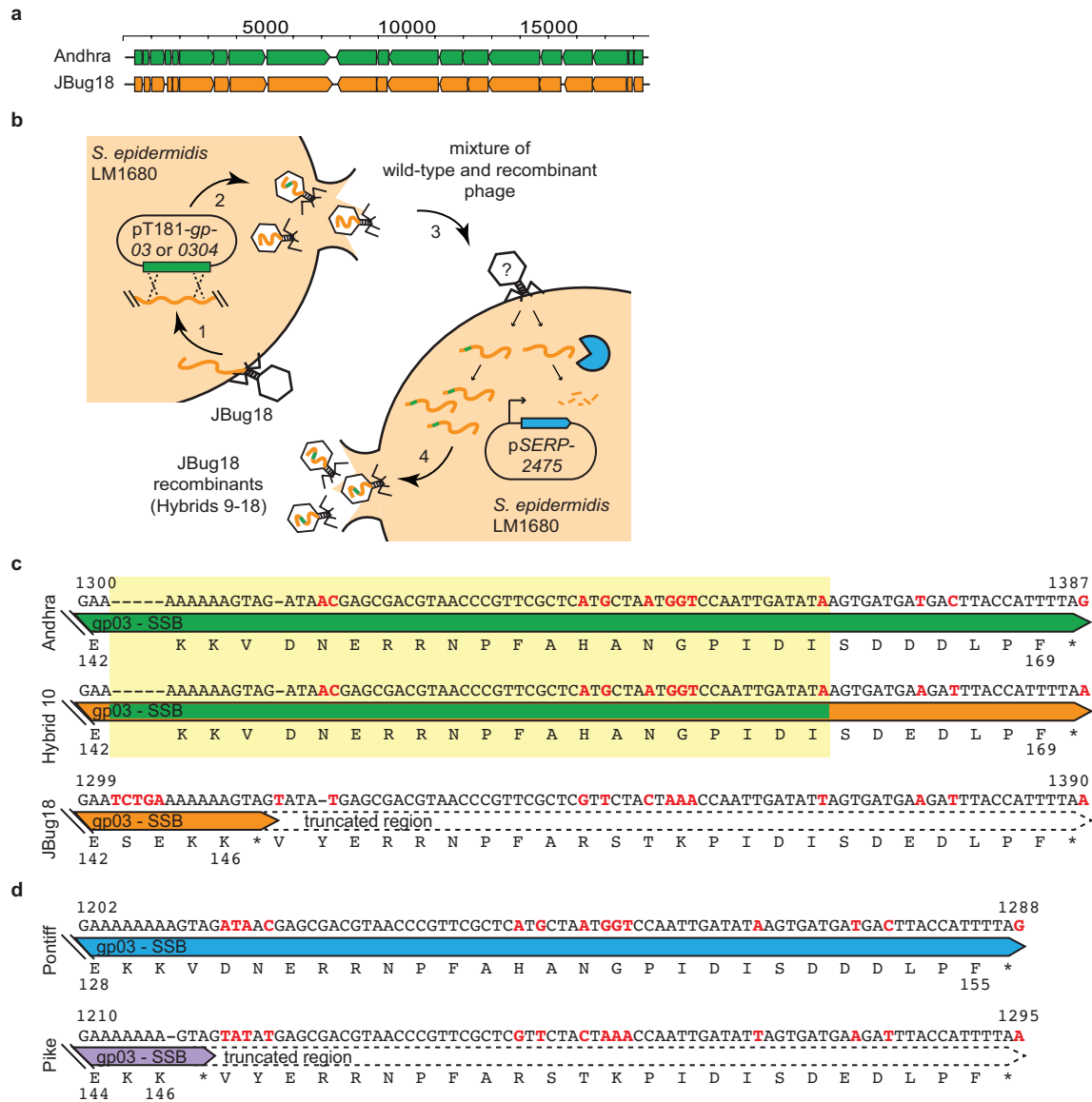
5' \*TCACTTGGTACTAAATTAATACTATGTGATACACGATTATATTTTC  
|||||  
AGTGAACCATGATTTAATTA

539

540

541

542 **Extended Data 7. Accompanies Fig. 2.** Sequences of DNA substrates used in nuclease and  
543 helicase assays in Fig. 2, panels (d) and (f). Asterisks indicate the position of the radiolabel.



544

545

546

547 **Extended Data 8. Accompanies Fig. 3. Generation of Hybrids 9-18 and comparison of**

548 **SSB sequences.** (a) A pairwise comparison of the open reading frames of Andhra and JBug18.

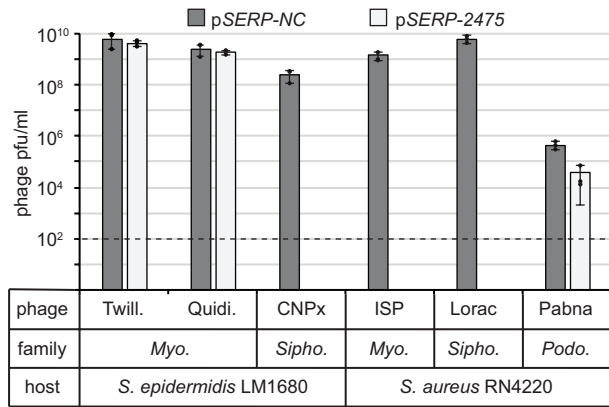
549 (b) A diagram of the method used to generate JBug18-Andhra Hybrids 9-18. (c) Sequence

550 comparison between the SSBs of Andhra, JBug18, and Hybrid 10, which gained resistance to

551 immunity through the acquisition of only 60 nucleotides of Andhra-derived sequence

552 (highlighted in yellow). (d) a similar comparison between the SSBs of phages Pontiff and Pike.





553

554

555

556

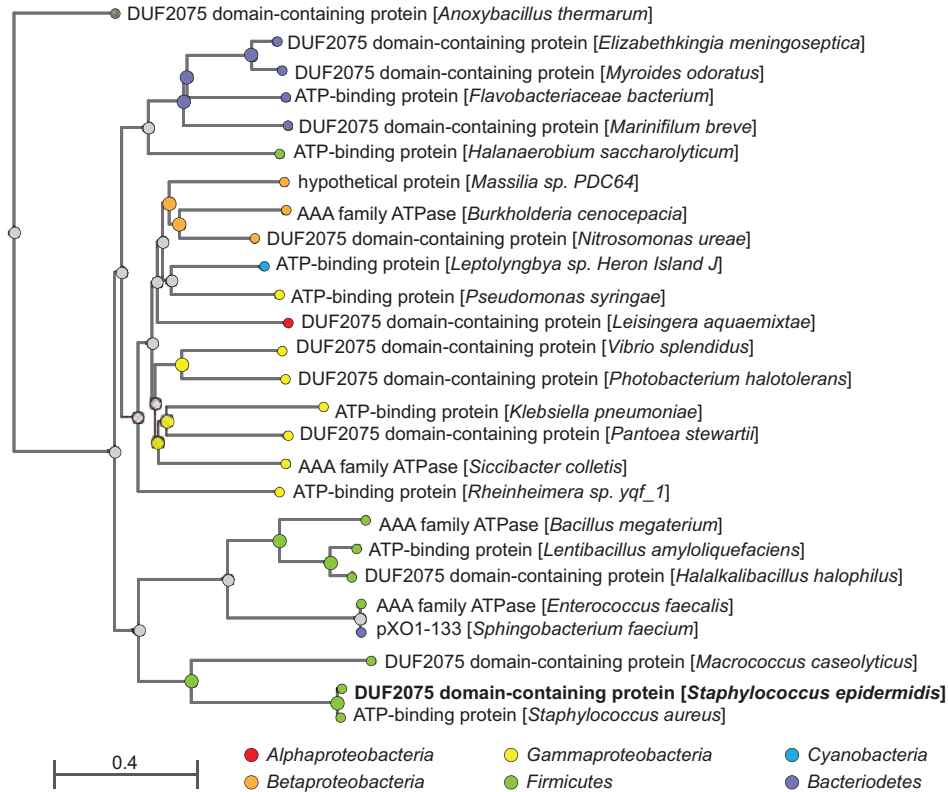
557 **Extended Data 9. SERP2475 protects against diverse staphylococcal phages.**

558 Staphylococcal strains bearing pSERP-NC or pSERP-2475 were plated together with indicated

559 phages. The resulting pfu/mL are shown as an average of triplicate measurements ( $\pm$ S.D.). The

560 dotted line indicates the limit of detection. Twill., Twilingate; Quidi., Quidividi; *Myo.*, *Myoviridae*;

561 *Sipho.*, *Siphoviridae*; *Podo.*, *Podoviridae*.



562

563

564

565

566

567 **Extended Data 10. SERP2475 homologs are found in diverse bacterial phyla. A**

568 phylogenetic tree constructed from the alignment of SERP2475 homologs found in 25

569 representative genera. All homologs selected share >30% sequence identity across >70% of

570 their protein sequence. The tree was generated using the NCBI BLAST tool

571 (<https://blast.ncbi.nlm.nih.gov/Blast.cgi>).